Reprinted from the *Journal of Environmental Quality*
Volume 29, no. 6, Nov.–Dec. 2000.
677 South Segoe Rd., Madison, WI 53711 USA

Denitrification Rates Predicted by Nitrogen-15 Labeled Nitrate Microcosm Studies, In Situ Measurements, and Modeling

Carl Christian Hoffmann,* Søren Rysgaard, and Peter Berg

ABSTRACT

Denitrification rates in the range of 359 to 599 mmol N m^{-2} d^{-1} were found in the waterlogged soil of a minerotrophic fen. Three different methods were used to estimate denitrification rates. The fen revealed a zone of enhanced denitrification and within this zone the spatial variation of denitrification rates was elucidated using two different approaches: microcosms and field observations. The denitrification rates in the microcosms were measured, either by use of ^{15}N–N_2 production rates (Method 1) or by setting up a mass balance for nitrate (Method 2). Denitrification rates in the peat horizon at depths of 0 to 69 cm were in the range 182 to 243 mmol N m^{-2} d^{-1} (Method 1) and 213 to 217 mmol N m^{-2} d^{-1} (Method 2). Denitrification rates measured in the deeper sandy soil horizons at depths of 69 to 156 cm were 46 to 103 mmol N m^{-2} d^{-1} (Method 1) and 33 to 137 mmol N m^{-2} d^{-1} (Method 2). Thus, both experiments revealed a strong and comparable decrease in denitrification rate with depth, which also corresponded well to soil carbon content. Denitrification rates were calcultaed from field data using Darcy's law and the conservation equation for one-dimensional, steady state, advective transport of nitrate in an incompressible porous medium. The same significant decrease in denitrification rates with depth was observed as in the microcosm setup. The calculated denitrification rates were: 330 mmol N m^{-2} d^{-1} at depths of 0 to 75 cm (peat), 20 mmol N m^{-2} d^{-1} at depths of 75 to 115 cm (sandy soil), and 9 mmol N m^{-2} d^{-1} in the sandy soil horizon at depths of 155 to 205 cm. This study shows that detailed spatial information about pedological and hydrological parameters in combination with detailed spatial mapping and measurement of denitrification rates is fundamental for properly understanding nitrogen removal in waterlogged soils with ground water through-flow. Further, the results confirm that provided this information is present, it is possible to compare detailed laboratory experiments with field studies of denitrification.

NATURAL riparian wetlands are often discharge areas for ground water to nearby streams (Lowrance et al., 1984). It has been documented that riparian wetlands are able to reduce nitrate concentration in ground water passing through the wetland (Peterjohn and Correll, 1984; Jacobs and Gilliam, 1985; Cooper, 1990; Haycock and Pinay, 1993; Pinay et al., 1993). Nitrate reduction seems to take place at high rates in a narrow zone often localized at the border between the upland and the wetland (Lowrance et al., 1984; Peterjohn and Correll, 1984; Cooper, 1990; Haycock and Pinay, 1993). Although field measurements have shown that nitrate disappears while tracing ground water flow lines, it has been difficult to demonstrate in the laboratory that nitrate is denitrified (Groffman et al., 1992, 1996; Lowrance, 1992; Nelson et al., 1995) and not removed by other processes (i.e., by microbial immobilization or by plant uptake). The main problem related to measuring actual denitrification in wetlands with ground water through-flow is that when collecting soil core samples, the ground water flow is cut off and with it the supply of nitrate by mass transport, leaving the nitrate supply to be dependent on diffusion alone. Infiltration experiments performed by Stepanauskas et al. (1996), using the ^{15}N technique and continuous flow soil cores where water was allowed to percolate through the columns, have shown that it is possible to achieve denitrification rates in the laboratory that are comparable with denitrification rates in the field.

The aims of this study were to (i) evaluate a new design of a continuous flow soil column–microcosm for measurements of denitrification rates under in situ conditions, (ii) compare the traditional mass balance approach with the ^{15}N method, (iii) compare the microcosm results with denitrification rates estimated from field data including hydraulic heads, hydraulic conductivities, and nitrate concentrations, and (iv) investigate and demonstrate high denitrification rates in a riparian wetland, as indicated by an earlier mass balance study.

MATERIALS AND METHODS

Study Site and Soil Sampling

The field study was conducted in a minerotrophic riparian fen at Voldby brook in the river Gjern catchment area, Jutland, Denmark (UTM 9°49′ E, 56°14′ N). The fen is recharged

Carl Christian Hoffmann, National Environmental Research Institute, Dep. of Streams and Riparian Areas, Vejlsøvej 25, 8600 Silkeborg, Denmark. Søren Rysgaard, National Environmental Research Institute, Dep. of Lake and Estuarine Ecology, Vejlsøvej 25, 8600 Silkeborg, Denmark. Peter Berg, Dep. of Environmental Sciences, Univ. of Virginia, Charlottesville, VA 22903. Received 21 Dec. 1999. *Corresponding author (cch@dmu.dk).

Published in J. Environ. Qual. 29:2020–2028 (2000).

by nitrate-rich ground water. At the hill slope and the adjacent 15 m of the fen, a nitrate reduction zone has previously been detected (Dahl, 1995; Paludan and Blicher-Mathiesen, 1996; Blicher-Mathiesen, 1998; Hoffmann, 1998). The ground water flow pattern is characterized by lateral flow in the hill slope, but at the foot of the hill slope the flow becomes upward, as mapped by hydraulic heads and further demonstrated by use of a bromide tracer (Dahl, 1995; Paludan and Blicher-Mathiesen, 1996; Blicher-Mathiesen, 1998; Blicher-Mathiesen et al., 1998). Thus, in the nitrate reduction zone most ground water is upwelling, and 90% of the ground water is discharged as surface water via two rivulets to the nearby Voldby brook (Dahl, 1995).

In the upwelling area, the soil profile consists of fibric and sapric peat at depths of 0 to 50 cm, superseded at depths of 50 to 200 cm by layers of medium-grained sand with bands of fibric peat and more coarse-grained material (sand, gravel, and pebbles). At 200 to 225 cm is a layer of coarse gravel and pebbles, and below there is a 100- to 150-cm-thick layer of Gyttja (fine grained lake sediment with organic content higher than 30%), which continues throughout the fen to the brook.

Hydraulic conductivities in the upwelling area were estimated by using installed piezometers for slug tests. The hydraulic conductivities were calculated according to Bouwer and Rice (1976).

Prior to soil sampling and start of the laboratory experiments, field measurements of hydraulic heads and sampling of ground water were undertaken from polyethylene piezometers with 10-cm-long screens installed at four depths, as shown in Fig. 1. The water levels in the piezometers were measured with a Plexiglas tube with a tape measure attached. The Plexiglas tube was further connected to a piece of flexible rubber tube. By blowing gently in the rubber tube and at the same time lowering the plexiglas tube into the piezometer until it reaches the water table, it is possible to make accurate measurements of the water level (±1 mm), simply by placing a fingernail at the lip of the piezometer tube and pressing it against the tape measure, exactly when the tongue senses air bubbles. The tops of the piezometers were leveled in order to convert water levels to hydraulic heads. Ground water was sampled with a submersible pump (Whale 921, Munster Simms Eng., Bangor, Northern Ireland) and samples were collected in polyethylene bottles. To ensure sampling of fresh ground water the piezometers were emptied the day before sampling. The ground water samples were stored at 5°C and analyzed the following day (for analytical procedures see below).

Undisturbed soil cores for use in the denitrification experiment in the laboratory were sampled from the upwelling area between Piezometer Nests 4 and 5 (Fig. 1). Soil sampling was performed with steel cylinders (50–60 cm long, 60-mm i.d.). The cylinders were sharpened at the bottom end and a specially designed iron head was constructed to fit inside the top of the cylinder. The cylinder was fastened to the iron head by screws. The iron head had a hole in the middle with a rubber washer and a steel washer at the top, allowing water and air to flow out of the cylinders as soil drilling and sampling went deeper and deeper into the wetland soil. The iron head was mounted to ordinary soil drilling equipment (Eijkelkamp, Giesbeek, the Netherlands). The same steel cylinders were used in the laboratory setup. Holes with a diameter of 5 mm were drilled in the wall of the steel cylinder at 3-cm intervals. During soil sampling, the holes in the steel cylinder were covered with waterproof tape. After sampling, the cylinders were sealed at both ends with rubber stoppers, stored in an upright position, and brought to the laboratory within 1 h.

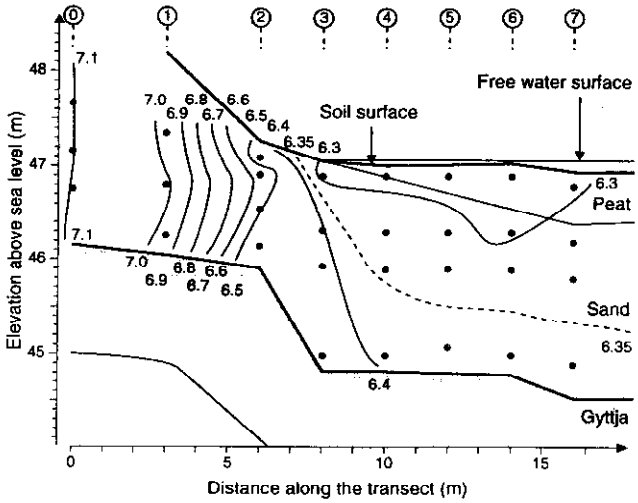

Fig. 1. Cross-section of the fen showing the hill slope recharging the fen with ground water and the upwelling area next to the hill slope. The hydraulic heads are shown as equipotential curves. The piezometer nests are labeled 0 to 7 at the top of the figure. ⊙ marks the position of screens of each of the piezometers. Length of screens is 10 cm.

Mathematical Formulation of the Transport and Removal of Nitrate

The hydraulic heads, hydraulic conductivities, and nitrate concentrations measured in the field were used to model and calculate the flow rate and the removal of nitrate along the almost- vertical flow lines in the upwelling area.

Excluding molecular diffusion and hydrodynamic dispersion (see discussion later) the conservation equation for a two-dimensional steady state transport of a solute in an incompressible porous medium can be written as (see Bear and Verruijt, 1987; Domenico and Schwartz, 1990):

$$q_x \frac{\partial C}{\partial x} + q_y \frac{\partial C}{\partial y} + R = 0 \qquad [1]$$

where q_x is the specific discharge in the horizontal x direction, q_y is the specific discharge in the vertical y direction, C is the concentration of NO_3^-, and R is the removal rate of NO_3^- per unit volume of soil. The equation can be approximated by the standard control volume discretization (Patankar, 1980):

$$q_{xi,j} \frac{C_{i+1/2,j} - C_{i-1/2,j}}{\Delta x_{i,j}} + q_{yi,j} \frac{C_{i,j+1/2} - C_{i,j-1/2}}{\Delta y_{i,j}} + R_{i,j} = 0 \qquad [2]$$

where i and j refer to the different positions in the x and y directions, respectively. As shown in our field measurements (see details later), the first term in Eq. [2] can be disregarded and a good estimate of the removal rate of NO_3^- can be calculated as:

$$R_{i,j} = -q_{yi,j} \frac{C_{i,j+1/2} - C_{i,j-1/2}}{\Delta y_{i,j}} \qquad [3]$$

The vertical specific discharges ($q_{y,\,i,\,j}$) are calculated from measured hydraulic heads ($\Phi_{i,j+1/2}$ and $\Phi_{i,j-1/2}$) and averaged hydraulic conductivities ($K_{i,j}$) using Darcy's law:

$$q_{yi,j} = -K_{i,j} \frac{\Phi_{i,j+1/2} - \Phi_{i,j-1/2}}{\Delta y_{i,j}} \qquad [4]$$

Labratory Experimental Setup

In the laboratory, the steel cylinders containing the soil samples were transformed into a microcosm setup. The waterproof tape covering the holes in the cylinder wall was replaced with butyl rubber fastened with hose clips. At both ends the cylinder was sealed with a hollow acrylic cap, lined with O-rings to make it gas-tight, and through tube connections piped to a water reservoir. The water reservoir consisted of a flexible airtight triple-walled plastic bag consisting of 80 μm nylon, 6.5 μm eval (ethylenevinylalcohol) and 100 μm polyethylene (Ril-O-Ten 80/100, Otto Nielsen Emballage, Aarhus, Denmark). The reservoir was further made height-adjustable in order to establish a similar hydraulic pressure in the core to that measured in situ (Fig. 2). The soil cores were set up in a climate chamber at 10°C with a continuous flow of ground water from the bottom to the top of each cylinder, as observed in the field. The outlet water was collected in a glass vial and the amount measured daily. In order to keep the system gas-tight, all tubing was Tygon tubing (Norton Performance Plastics, Akron, OH) (Fig. 2). Due to the direction of flow, a stainless steel cross was mounted at the soil surface at the top of each of the cylinders to prevent the core from being displaced by the hydraulic pressure applied to the core by the water reservoir. Sampling of water and soluble gases took place from the inlet and outlet of the cylinders through valves and from the butyl-covered holes by use of syringes. Injection needles (1.20 × 40 mm) were permanently mounted in the core and covered with small rubber stoppers between periods of sampling. The ground water used in the study was collected in the fen from a piezometer close to the soil sampling point. Before use, the ground water was flushed for 30 min with helium gas to make sure that it was kept anoxic as in the field. To check whether the water was distributed uniformly throughout the soil columns, bromide was added to the inlet water. Furthermore, water samples from the plastic bag and the inlet tube were analyzed every day for dissolved oxygen by Winkler titration (Fenchel and Hemmingsen, 1974) in order to check that the system was gas tight. At the end of the laboratory experiment, mass loss on ignition was determined in 10-cm sections of the soil cores.

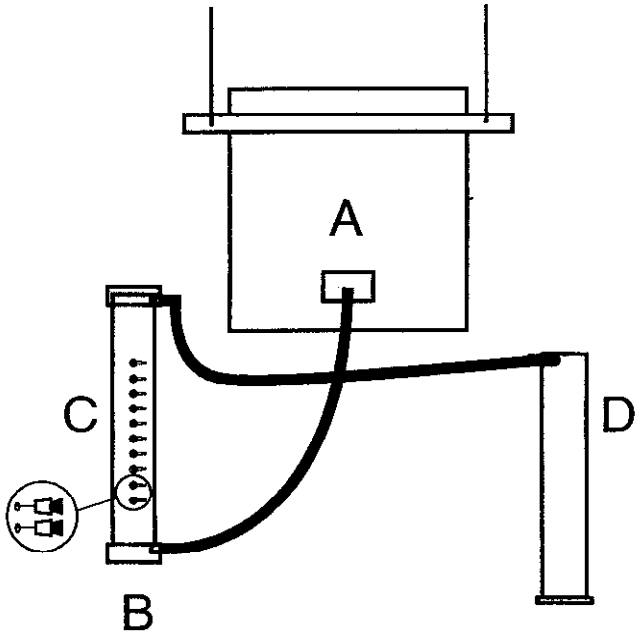

Fig. 2. Experimental setup of the microcosms, showing (*A*) the gas-tight water reservoir, from which water as a result of the pressure difference (hydraulic head) is forced through (*C*) the column from the bottom (*B*) to the top and out in the measuring glass (*D*). The enlarged circle shows needles (covered with rubber stoppers) inserted through butyl rubber septa.

Preincubation, Sampling of Nitrate and Bromide, and Checking Stability of Soil Columns

The four microcosms (0 to 42, 42 to 69, 69 to 111, and 111 to 156 cm) were run for more than 2 mo, starting 31 Oct. 1995 and ending in January 1996. The first 2 wk were used to check the stability of the columns. Flow rates were measured every day. The concentration of bromide was monitored to see if it was evenly distributed throughout the columns and the nitrate concentrations and nitrate reduction were analyzed to evaluate the stability of the nitrate profile. After 2 wk, new water reservoirs containing $^{15}NO_3^-$-enriched ground water were initiated. The initial measurements of flow rate as well as the bromide results were used to estimate when sampling of ^{15}N could proceed. The columns were flushed several times with $^{15}NO_3^-$–labeled water before sampling was started. After approximately 10 to 15 d, depending on flow rate, the columns were exposed to nonlabeled ground water again and the nitrate concentrations in the four columns were monitored the next 4 wk either by measuring inflow and outflow concentrations or by making detailed vertical profiles.

For determination of the concentrations of NO_2^-, NO_3^-, and Br^-, 2-mL filtered water samples (Whatman GF/C glass fiber filters) were collected through the butyl rubber septa with a syringe and stored in glass vials at 5°C until analysis, which took place within a few hours after sampling, or the following day.

The concentrations of NO_2^- and $NO_2^- + NO_3^-$ were analyzed on a flow-injection analyzer (QuikChem automated ion analyzer, Lachat Instruments, Milwaukee, WI) with Method 10-107-04-1-B (Lachat Instruments, 1989). Bromide and NO_3^- (concentration >70 μ*M* NO_3^-–N) were determined by ion chromatography on a Shimadzu HIC-6A, equipped with an IC-A1S anion column (Shimadzu, Kyoto, Japan), at a flow rate of 1.5 mL min^{-1} and with 2.5 m*M* phthalic acid at pH 4.0 as an eluent. Samples for ion chromatography were filtered through 0.2-μm cellulose acetate membrane filters (Micro Filtration Systems, Osmonics, West Borough, MA).

Sampling and Determination of Nitrogen-15

To the collected ground water containing 1.5 m*M* NO_3^-, 0.35 m*M* $Na^{15}NO_3$ (99.8% ^{15}N, Europa Scientific, Crewe, UK) was added, resulting in a final NO_3^- concentration of 1.85 m*M* and a ^{15}N atom% of approximately 20. The resulting NO_3^- concentration was within the range of NO_3^- concentrations found in the ground water at the hill slope that enters the fen area (Dahl, 1995; Blicher-Mathiesen, 1998; Hoffmann, 1998). The ^{15}N-enriched ground water was used as inflow water to the four soil columns.

One-milliliter samples for ^{15}N determination were collected by syringe through the butyl rubber septa in the cylinder wall and injected into 6.6-mL helium-flushed glass vials (Exetainer, Labco, High Wycombe, UK) and 0.2 mL of a $ZnCl_2$ solution (50% w/v) was added to stop bacterial activity. The glass vials were weighed before and after sampling to determine the exact amount of sample. After sampling, the glass vials were shaken vigorously for 5 min to equilibrate the N_2 gas between the water and helium gas phase. The entire helium gas phase was injected into a gas chromatograph coupled to a triple-collector isotopic ratio mass spectrometer (RoboPrep-G^+ in

Table 1. Measured (9 Oct. 1995) hydraulic heads and hydraulic conductivities in piezometer nests at Stations 2, 3, 4, 5 and 6.

Piezometer	Station 2	Conductivity	Station 3	Conductivity	Station 4	Conductivity	Station 5	Conductivity	Station 6	Conductivity
nest	m	m d^{-1}	m	m d^{-1}	m	m d^{-1}	m	m d^{-1}	m	m d^{-1}
1	–		6.29	0.40	6.29	7.30	6.29	18.92	6.29	11.74
2	–		6.41	3.28	6.34	2.23	6.31	3.11	6.29	3.21
3	6.50	3.28	6.41	3.34	6.36	2.31	6.32	8.26	6.33	8.43
4	–		6.46	3.80	6.39	2.31	6.38	3.43	6.37	2.48

line with TracerMass, Europa Scientific) and the abundance and concentration of $^{14}N^{15}N$ and $^{15}N^{15}N$ analyzed. Further details are given in Risgaard-Petersen and Rysgaard (1995). The ^{15}N isotopic distribution in the NO_3^- pool was likewise analyzed by mass spectrometry after reducing NO_3^- to N_2 using a denitrifying culture (Risgaard-Petersen et al., 1993). Rates of denitrification were calculated using the isotope pairing technique described by Nielsen (1992).

Nitrate consumption and N_2 production rates were calculated from the difference in concentration at the inflow and at the depth investigated, taking into account the area of the cylinder and the flow rate.

RESULTS

Ground Water Flow

The ground water flow pattern derived from the measured hydraulic heads showed a lateral flow at the hill slope and upwelling of ground water in the fen area next to the hill slope. The flow pattern is shown as equipotential curves in Fig. 1. The measured hydraulic heads in the upwelling area (see Table 1) were used to calculate the horizontal and the vertical flow rates from Darcy's law. The calculated hydraulic conductivities from the slug tests were used in the model (Table 1). The average hydraulic conductivities between the piezometer nests were calculated as arithmetic means. The calculated flow rates from 9 Oct. 1995 are illustrated in Fig. 3 as vectors, where the lengths of the vectors represent the sizes of the flow rates. It is evident that the main flow direction in the upwelling area was vertical and pointing toward the surface of the fen. Almost identical flow patterns were found on two other dates (13 June 1995 and 22 Aug. 1995; data not shown).

Nitrate Removal

Field measurements of nitrate, collected 9 Oct. 1995, reveal that nitrate concentrations decrease along the transect both in the horizontal and vertical direction in the upwelling area next to the hill slope (Fig. 4). At the hill slope the concentration of nitrate was in the range 1.41 to 1.56 mM, but 16 m further out in the fen at Station 7, all NO_3^- disappeared or decreased to trace amounts. The concentrations of NO_3^- and NH_4^+ in surface water at Piezometer Nest 7 were 2.1 and 2.3 μM, respectively.

As expressed in Eq. [2], the removal rate of nitrate (R) is a function of the flow rates and concentration gradients in the x and y directions, respectively. On average, both the concentration gradients and the flow rates are significantly higher in the y direction than in the x direction, allowing us to disregard the contribution from the x direction when estimating values of R (Eq. [3]). The validity of this simplification was confirmed by calculating the contributions for the two directions using the data in Fig. 3 and 4, which gave an average contribution of 0.17 ± 0.07 μmol N cm^{-3} d^{-1} ($\pm$SE, n = 9) for the y direction and -0.0081 ± 0.0042 μmol N cm^{-3} d^{-1} ($\pm$SE, n = 8) for the x direction. The value for the x direction is not significantly different from zero. The same pattern was found using data from 13 June 1995 and 22 Aug. 1995 (data not shown).

The removal rates of nitrate were calculated from Eq. [3] for Stations 3, 4, and 5 and averaged over the three depth intervals from 15 to 75, 75 to 115, and 115 to 205 cm. The mean values from 9 Oct. 1995 are given in Fig. 5, showing a significant decrease with depth. In the

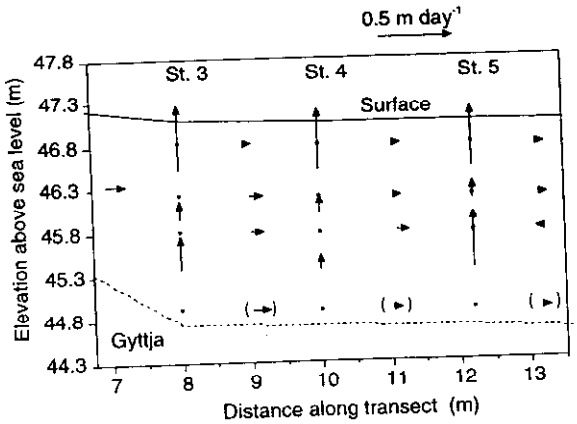

Fig. 3. Calculated flow vectors in the upwelling area.

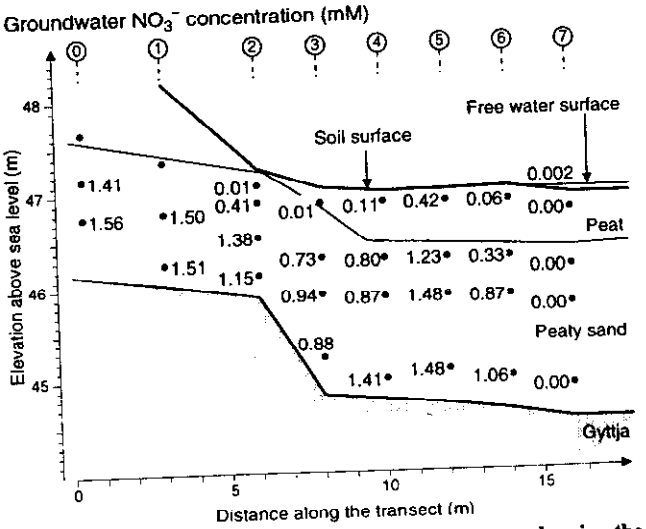

Fig. 4. Cross-section of the fen showing the hill slope recharging the fen with nitrate-rich ground water and the upwelling area next to the hill slope. The figures show the nitrate concentration measured at each piezometer at each of the nests, which are labeled 0 to 7 at the top of the figure. ⊙ marks the position of screens of each of the piezometers. Length of screens is 10 cm.

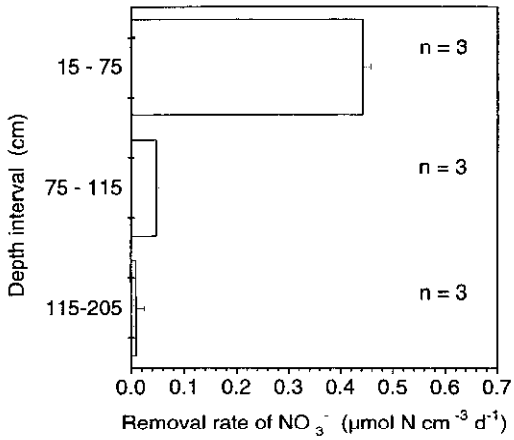

Fig. 5. Nitrate removal rates in the upwelling area averaged for three depth intervals.

upper 15 to 75 cm of the fen, nitrate concentrations were reduced from 0.92 to 0.17 m*M* NO_3^- on average, which is equivalent to a denitrification rate of 0.44 ± 0.02 μmol N cm^{-3} d^{-1} (±SE). The rates from 13 June 1995 and 22 Aug. 1995 show the same strong variation with depth and comparable rates of 0.38 ± 0.07 and 0.51 ± 0.07 μmol N cm^{-3} d^{-1}, respectively, in the 15- to 75-cm depth interval. The estimated rate in the 75- to 115-cm depth interval was equal to 0.05 ± 0.03 μmol N cm^{-3} d^{-1} (Fig. 5), which is almost a factor of 10 smaller than the rate in the upper depth interval. In the lower depth interval, from 115 to 205 cm, the rate was close to zero (i.e., 0.0096 ± 0.01162 μmol N cm^{-3} d^{-1}). The total depth integrated denitrification rate (0–205 cm) was 359 mmol N m^{-2} d^{-1} (assuming the same denitrification rate at depths of 0–15 cm as at depths of 15–75 cm, Fig. 5).

Laboratory Experiments

The mean flow rates in the microcosms measured during the laboratory experiment varied from 11.5 mL cm^{-2} d^{-1} at depths of 0 to 42 cm to 16.5 mL cm^{-2} d^{-1} at depths of 69 to 111 cm (Table 2). Flow rates of Cores 1, 2, and 4 were not significantly different ($p < 0.05$, Student's paired *t*-test) from each other, whereas the flow rate of Core 3 was significantly different from the flow rates in Cores 1 and 2 ($p < 0.05$).

The ^{15}N concentration profiles within the soil cores, expressed as $^{29}N_2$ ($^{14}N^{15}N$) and $^{30}N_2$ ($^{15}N^{15}N$), increased from the bottom to the top of the soil (Fig. 6). In the deepest soil core (111–156 cm) the sum of the concentrations of $^{29}N_2$ and $^{30}N_2$ was up to 57 μ*M*. In the 69- to 111-cm soil core the concentration of ^{15}N-labeled N_2 began to increase at a depth of 96 cm and gradually rose toward the top at a depth of 70 cm (outlet), reaching a level of 113 μ*M* ($^{29}N_2$ + $^{30}N_2$). In the 42- to 69-cm soil core the concentration of ^{15}N-labeled N_2 increased gradually from 0.4 μ*M* ($^{29}N_2$ + $^{30}N_2$) at a depth of 69 cm to 297 μ*M* ($^{29}N_2$ + $^{30}N_2$) at a depth of 48 cm. At this depth, all NO_3^- was depleted from the porewater (see Fig. 6 and 7). The soil core representing the topsoil showed a rapid increase in ^{15}N-labeled N_2 concentration from the inlet side at a depth of 42 cm, 0.2 μ*M* ($^{29}N_2$ + $^{30}N_2$), to a depth of 36 cm, 240 μ*M* ($^{29}N_2$ + $^{30}N_2$), after which the concentration only increased slightly because most nitrate had been reduced.

Table 2. Flow rates for the four soil cores (*n* = 11).

Core	Depth	Flow rate (±SE)
	cm	mL cm^{-2} d^{-1}
1	0–42	11.5 ± 2.1
2	42–69	12.1 ± 1.9
3	69–111	16.5 ± 1.9
4	111–156	14.2 ± 1.6

Nitrate concentrations measured by standard methods showed exactly the reverse concentration pattern (Fig. 7), as can be deduced from the ^{15}N measurements (Fig. 6) (i.e., with increasing N_2 production the nitrate concentration simultaneously decreased).

Calculation of the denitrification rates measured either as ^{15}N production or as NO_3^- consumption with the standard method is shown for each of the four columns in Table 3. Although there are minor differences in calculated denitrification rates between the two approaches, the overall results are essentially identical. The small differences in rates probably reflect day to day variation in hydraulic load and consequently nitrate load, as sampling of water for analysis took place only once a day (i.e., samples for ^{15}N measurements were taken one day and samples for nitrate determination by standard methods the next day).

Calculation of the specific denitrification rate at each of the measured depths showed that the denitrification rate tended to increase from the bottom to the top of the fen soil (Fig. 8). In the two cores with soil from depths of 111 to 156 and 69 to 111 cm, respectively, there was no denitrification in the horizons with a low loss on ignition (i.e., <3%). However, in the upper part of Core 4 (Fig. 8) at depths of 114 to 123 cm, denitrification took place at comparatively high rates (mean 111–156 cm = 0.10 ± 0.05 μmol N_2–N cm^{-3} d^{-1} or 0.07 ± 0.04 μmol N_2–N g dry $wt.^{-1}$ d^{-1}; bulk density 1.31). At depths of 69 to 111 cm, the denitrification rate was 0.24 ± 0.09 μmol N_2–N cm^{-3} d^{-1}, which equals 0.19 ± 0.07 μmol N_2–N g dry $wt.^{-1}$ d^{-1} (bulk density 1.27–1.31). In the soil column (2) covering the depth interval from 42 to 69 cm, the denitrification rate was 0.87 ± 0.22 μmol N_2–N cm^{-3} d^{-1} (0.68 ± 0.17 μmol N_2–N g dry wt. $^{-1}$ d^{-1}; bulk density 0.63–1.27) as long as NO_3^- was still present (i.e., until a depth of 48 cm). In the uppermost part of the soil the denitrification rate was high at depths of 36 to 42 cm, reaching a maximum of 3.3 μmol N_2–N cm^{-3} d^{-1} at a depth of 36 cm, followed by a steep decrease due to depletion of NO_3^-. At depths of 27, 18, and 12 cm, high specific denitrification rates were observed (Fig. 8), but inbetween, at depths of 21 to 24 and 12 to 15 cm, the activity was very small (~0.02 μmol N_2–N cm^{-3} d^{-1}). This may have been due to a microscale preferential flow mechanism (e.g., a dead rhizome forming a tube funnelling water upward, thereby preventing contact between nitrate, water, and the surrounding soil matrix). At depths of 12 to 39 cm, where

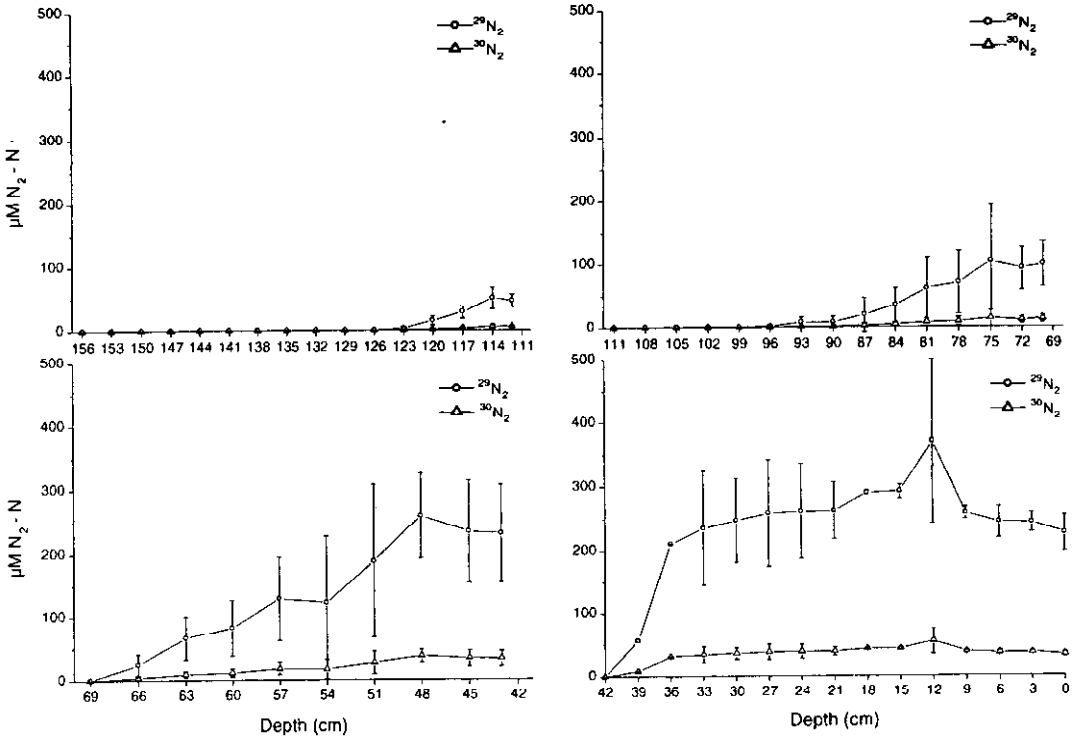

Fig. 6. The isotopes $^{29}N_2$ and $^{30}N_2$ measured in the four columns measured at the inlet, outlet, and for every 3 cm along the cylinder walls through butyl rubber septa. The direction is from 156 to 0 cm (i.e., Column 4: 156 to 111 cm, Column 3: 111 to 69 cm, Column 2: 69 to 42 cm, and Column 1: 42 to 0 cm).

nitrate was still present in the porewater, the mean denitrification rate was 0.80 ± 0.33 μmol N_2–N cm^{-3} d^{-1}, but due to the low bulk densities (0.08–0.63) in this organic soil, the rate of denitrification expressed on a dry weight basis was somewhat higher, 4.50 ± 2.05 μmol N_2–N g dry $wt.^{-1}$ d^{-1}. The total depth integration (using

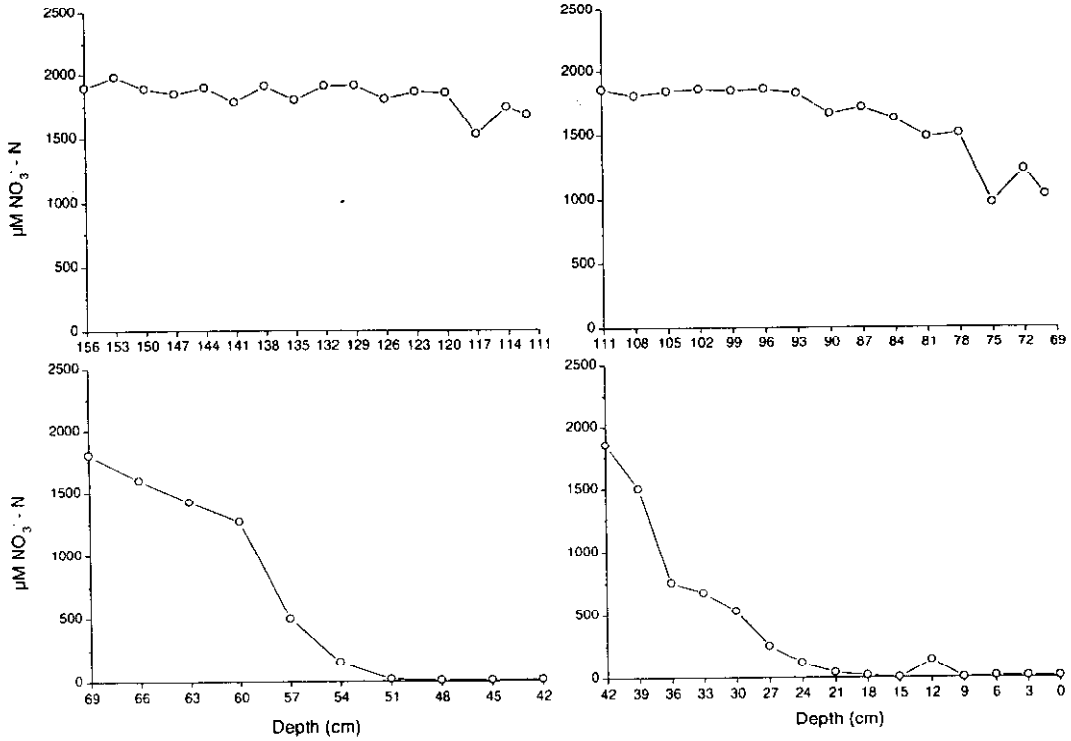

Fig. 7. Nitrate concentration measured at inlet, outlet, and for every 3 cm along the cylinder wall in each of the four columns. The direction of flow is from 156 to 0 cm.

Table 3. Denitrification rates and nitrate reduction rates integrated from bottom to top for each of the four microcosms and overall. Values are given in mmol N m^{-2} d^{-1} and in parentheses as grams N m^{-2} d^{-1}.

Column number	Depth	^{15}N method	Standard method
	cm	— mmol N m^{-2} d^{-1} (g N m^{-2} d^{-1}) —	
1	0–42	243.0 (3.4)	212.6 (3.0)
2	42–69	181.7 (2.5)	216.8 (3.0)
3	69–111	102.7 (1.4)	136.7 (1.9)
4	111–156	45.7 (0.6)	32.9 (0.5)
Total		573.1 (7.9)	599.0 (8.4)

the trapezoidal rule) of the denitrification rates for all four microcosms amounted to 573 mmol N m^{-2} d^{-1} (Table 3). The same calculation using the standard method (i.e., decrease in nitrate concentration) gave 599 mmol N m^{-2} d^{-1}, which is very similar to the ^{15}N method (Table 3).

DISCUSSION

The ground water flow pattern characterized by lateral flow at the hill slope and upwelling of ground water in the fen area next to the hill slope has previously been reported by Dahl (1995), Blicher-Mathiesen et al. (1998), and Hoffmann (1998). We believe that the upward flow is fed by water from the layer of coarse gravel and pebbles located immediately on top of the Gyttja layer. Since this gravel layer has a hydraulic conductivity that is assumed to be orders of magnitude higher than conductivities for other parts of the area, high flow rates are expected, and we believe that the calculated horizontal flow rates for the lowest nests (Fig. 3, arrows in parentheses) are not representative of this depth interval. Based on the soil characteristics it is reasonable to assume that the Gyttja layer can be regarded as relatively impermeable (i.e., with a hydraulic conductivity around 10^{-10} m s^{-1}; Döll and Schneider, 1995), but this is not necessarily correct. With the topography to the left of the upwelling area, large potential gradients are expected over the Gyttja layer, which could lead to vertical flow across this layer. However, measurements in additional piezometer nests penetrating the Gyttja layer between Stations 3 and 5 show that the nitrate concentrations here are close to zero (data not shown). The high nitrate concentrations that are found directly above the Gyttja layer (Fig. 4) indicate that there is no significant transport across the Gyttja layer.

In our estimates of denitrification rates from the field data (Eq. [3]) we assumed that advection was the dominant form of transport while molecular diffusion and hydrodynamic dispersion were insignificant. The magnitude of hydrodynamic dispersion compared with molecular diffusion can be evaluated from the Peclet number (Pe), defined as $(q_y d_m)/(nD_d)$ where d_m is the mean grain-size of the soil, n is the porosity, and D_d is the molecular diffusivity of NO_3^- in water (Bear and Verrujit, 1987 or Domenico and Schwarz, 1990). With a mean specific discharge (q_y) of 3×10^{-4} cm s^{-1} (calculated from the field data), estimated values for d_m and n of 0.01 cm and 0.5, respectively, and a value of D_d of 13×10^{-6} cm^2 s^{-1} (~10°C; Li and Gregory, 1974), Pe can be calculated to be 0.4. At this Pe value, hydrodynamic dispersion is smaller than, or has the same magnitude, as molecular diffusion (Bear and Verruijt, 1987; Domenico and Schwartz, 1990). With a mean concentration of 900 nmol cm^{-3} and a mean concentration gradient of −6 nmol cm^{-4} (both calculated from the field data), the magnitude of the advective flux ($-q_y C$) was a factor of approximately 3000 larger that the molecular diffusive flux ($\sim -D_d dC/dy$, not corrected for tortuosity). This analysis shows that the transport of NO_3^- by molecular diffusion and hydrodynamic dispersion clearly was insignificant compared with advection.

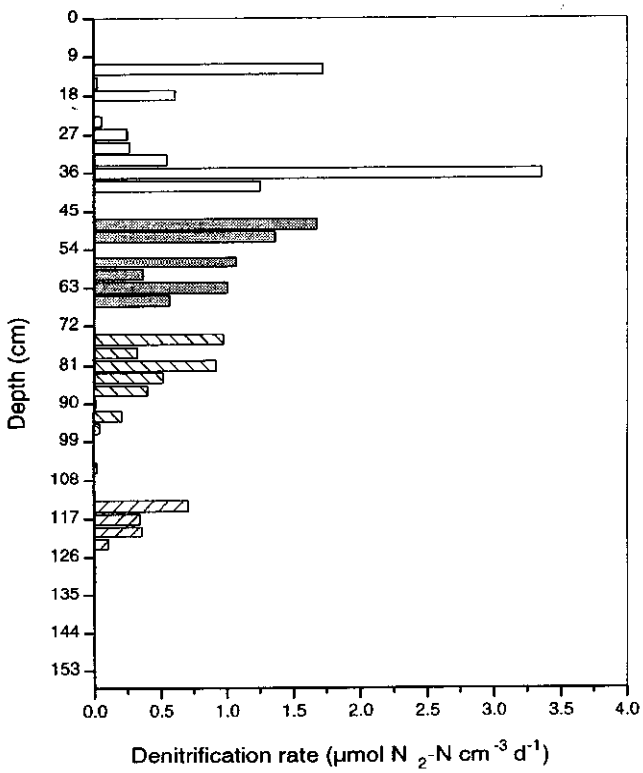

Fig. 8. Calculated denitrification rates in µmol N_2–N cm^{-3} d^{-1} using ^{15}N data from the four microcosms.

Comparing the specific denitrification rates obtained from the laboratory microcosm study with the nitrate removal rates calculated from the field data shows good accordance at depths of 15 to 75 cm. The field rates varied between 0.38 and 0.51 µmol N cm^{-3} d^{-1} on different dates. Taking the lower nitrate concentration level in the field into account, these rates roughly match the result of the microcosm studies, which gave a mean rate of 0.58 ± 0.17 µmol N cm^{-3} d^{-1}. At depths of 75 to 115 cm, the mean denitrification rate in the microcosm was 4.5 times higher than the nitrate removal rate from the field study (0.225 vs. 0.050). Also at depths of 115 to 205 cm, the mean denitrification rate in the microcosm was higher than the nitrate removal rate in the field (i.e., 0.0584 vs. 0.0096) as the latter is not significantly different from 0 (note: in the microcosm core denitrification measurements were only performed to a depth of 156 cm). These differences are presumably a result of differences in carbon availability and carbon content

Table 4. Loss on ignition (n = 2).

Depth	Loss on ignition
cm	%
0–10	68.4
10–30	18.5
30–68	11.3
68–78	12.0
78–88	13.0
88–98	3.0
98–112	1.6
112–122	9.2
122–132	0.5
132–142	0.6
142–153	1.0

between the soil in the microcosm and in the field, as the microcosms at depths of 68 to 153 cm had a varying organic content (Table 4), and the narrow bands of organic material (i.e., fibric peat) may not be evenly distributed throughout the upwelling area (differences in nitrate concentration are discussed below). In this context, the microcosm experiment also implies that denitrification in the deeper soil strata (i.e., 123 to 156 and 96 to 111 cm) is limited by carbon. The lack of ^{15}N-labeled N_2 at these depths is concomitant with low loss on ignition (<3%), while the depths with significant denitrification activity have a higher loss on ignition (>9%, Table 4).

The denitrification rates in the microcosms (573–599 mmol N m^{-2} d^{-1}) exceed the rate of nitrate reduction found from field data (359 mmol N m^{-2} d^{-1}). In the field denitrification took place in the two deepest soil columns (45.7 and 102.7 mmol N m^{-2} d^{-1}, respectively: some nitrate is reduced before reaching the upper soil strata), whereas all four columns were exposed to the same high initial nitrate concentration in the laboratory. In Microcosm 2, representing depths of 42 to 69 cm, all nitrate was reduced (at a depth of 51 cm) before reaching the outlet, which implies that the denitrification capacity in the fen is significantly higher. In principle, the uppermost part of the soil profile (Microcosm 1, depth 0–42 cm) is not necessary for the complete reduction of nitrate, but might instead be regarded as the excess denitrification capacity. Addition of the denitrification rates from the three lower microcosms (i.e., depth 42 to 156 cm) yields an integrated denitrification rate of 45.7 + 102.7 + 181.7 = 390 mmol N m^{-2} d^{-1}, which is in accordance with the calculated field rate of 359 mmol N m^{-2} d^{-1}. Furthermore, the initial nitrate concentration in the laboratory experiment was higher than in the field study (i.e., 1.8 to 1.9 vs. 1.4 to 1.6 mM NO_3^-). The field study also reveals that some nitrate is reduced, especially in the upper part of the soil at the hill slope, just before ground water enters the upwelling area. This observation has been confirmed by Blicher-Mathiesen (1998).

The mean denitrification rate of 4.50 ± 2.05 μmol N_2–N g dry wt.$^{-1}$ d^{-1} measured in the column (1) with the highest denitrification rate is somewhat higher than the highest mean rates of 0.40 to 0.65 μmol N_2O–N g dry wt.$^{-1}$ d^{-1} measured by Pavel et al. (1996) in a similar experiment where ground water was also admitted to the bottom of vertically positioned soil columns. Furthermore, the results of Pavel et al. (1996) could not be demonstrated in the field (Willems et al., 1997), probably because the local hydrological conditions such as ground water flow pattern and hydraulic conductivity did not favor high denitrification rates.

The denitrification rates measured in this study, both in the laboratory and in the field, are among the highest reported. Other studies have shown denitrification rates in the range of 3.6 to 52.9 mmol NO_3^-–N m^{-2} d^{-1} (Pinay and Decamps, 1988; Cooper, 1990; Brüsch and Nilsson, 1990; Fustec et al., 1991; Haycock and Burt, 1993; Pinay et al., 1993). Haycock and Pinay (1993) found that nitrate reduction rates, dependent on nitrate load, were up to 643 to 715 mmol NO_3^-–N m^{-2} d^{-1} (9–10 g NO_3^-–N m^{-2} d^{-1}), with a nitrate reduction efficiency of 100 and 84% for a riparian poplar site and a rye grass site, respectively. Furthermore, Schipper et al. (1993) found high denitrification rates (80 mmol NO_3–N m^{-2} d^{-1}) in an organic riparian soil receiving ground water from a spray site irrigated with sewage.

The high denitrification rates measured in both of the laboratory experiments in the present study show that the capacity for nitrogen removal in the investigated riparian fen is higher than the actual nitrogen removal calculated from the field measurements. However, as discussed above, this is partly due to NO_3^- concentrations in the field being different from those in the laboratory setup. The NO_3^- flowing vertically upward through the soil columns is reduced to N_2 by denitrifying bacteria in the deeper soil strata, reducing the NO_3^- concentration before it reaches the higher-capacity denitrification zones closer to the soil surface. This implies that the fen area, even at higher inflow NO_3^- concentrations, will have the capacity to remove NO_3^- before it reaches the outlet and is discharged to the brook. The high nitrogen removal rates measured in this study are also in agreement with a simple input–output mass balance calculated for the whole fen area in 1993; taking the upwelling area into account as a zone of enhanced denitrification activity. The calculated nitrate reduction rate was 336 mmol N m^{-2} d^{-1} (Hoffmann, 1998). Thus, the present study confirms that riparian wetland areas represent active sites of nitrogen removal, and our direct laboratory experiments further support that the NO_3^- removed is reduced to N_2 by bacterial denitrification.

In general, the results indicate that freshwater riparian wetlands exhibit a considerable potential for nitrate removal through denitrification, and thus restoration or rewetting of reclaimed freshwater wetlands with ground water through-flow may be an important tool for reducing nonpoint-source nitrogen pollution of the aquatic environment.

ACKNOWLEDGMENTS

The National Environmental Research Programme funded this study. We greatly acknowledge the technical assistance of Birte Eriksen, Egon Frandsen, and Dorte Nedergaard.

REFERENCES

Bear, J., and A. Verruijt. 1987. Modeling groundwater flow and pollution. Kluwer Academic Publ., Dordrecht, the Netherlands.

Blicher-Mathiesen, G. 1998. Kvælstoffjernelse i enge. (In Danish.)

Ph.D. diss. Aarhus Univ. and National Environ. Res. Inst., Silkeborg, Denmark.
Blicher-Mathiesen, G., G.W. McCarty, and L.P. Nielsen. 1998. Denitrification and degassing in groundwater estimated from dissolved dinitrogen and argon. J. Hydrol. 208:16–24.
Bouwer, H., and R.C. Rice. 1976. A slug test for determining hydraulic conductivity of unconfined aquifers with completely or partially penetrating wells. Water Resour. Res. 12:423–428.
Brüsch, W., and B. Nilsson. 1990. Nitrate turnover and water movement in a wetland. p. 241–258. *In* Anonymous (ed.) NPo-forskning fra Miljøstyrelsen, C-abstracts, nitrogen and phosphorus in fresh and marine waters. National Environ. Protection Agency, Copenhagen, Denmark.
Cooper, A.B. 1990. Nitrate depletion in the riparian zone and stream channel of a small headwater catchment. Hydrobiologia 202:13–26.
Dahl, M. 1995. Flow dynamics and water balance in two freshwater wetlands. Ph.D. diss. Univ. of Copenhagen and National Environ. Res. Inst., Silkeborg, Denmark.
Domenico, P.A., and F.W. Schwartz. 1990. Physical and chemical hydrogeology. John Wiley & Sons, New York.
Döll, P., and W. Schneider. 1995. Lab and field measurements of the hydraulic conductivity of clayey silts. Ground Water 33:884–891.
Fenchel, T., and B.B. Hemmingsen. 1974. Manual of microbial ecology. Academic Press, Copenhagen, Denmark.
Fustec, E., A. Mariotti, X. Grillo, and J. Sajus. 1991. Nitrate removal by denitrification in alluvial ground water: Role of a former channel. J. Hydrol. 123:337–354.
Groffman, P.M., A.J. Gold, and R.C. Simmons. 1992. Nitrate dynamics in riparian forests: Microbial studies. J. Environ. Qual. 21:666–671.
Groffman, P.M., G. Howard, A.J. Gold, and W.M. Nelson. 1996. Microbial nitrate processing in shallow groundwater in a riparian forest. J. Environ. Qual. 25:1309–1316.
Haycock, N.E., and T.P. Burt. 1993. Role of floodplain sediments in reducing the nitrate concentration of subsurface run-off: A case study in the Cotswolds, UK. Hydrol. Process. 7:287–295.
Haycock, N.E., and G. Pinay. 1993. Groundwater nitrate dynamics in grass and poplar vegetated riparian buffer strips during winter. J. Environ. Qual. 22:273–278.
Hoffmann, C.C. 1998. Nutrient retention in riparian wet meadows and fens. Ph.D. diss. Univ. of Copenhagen, Freshwater-Biological Lab. and National Environ. Res. Inst., Dep. of Streams and Riparian Areas, Silkeborg, Denmark.
Jacobs, T.C., and J.W. Gilliam. 1985. Riparian losses of nitrate from agricultural drainage waters. J. Environ. Qual. 14:472–478.
Lachat Instruments. 1989. QuickChem Method no. 10-107-04-1-B, nitrate + nitrite, nitrite, surface water. Lachat Instruments, Milwaukee, WI.
Li, Y.-H., and S. Gregory. 1974. Diffusion of ions in sea water and in deep-sea sediments. Geochim. Cosmochim. Acta 38:703–714.
Lowrance, R. 1992. Groundwater nitrate and denitrification in a coastal plain riparian forest. J. Environ. Qual. 21:401–405.
Lowrance, R.R., R.L. Todd, J. Fail, Jr., O. Hendrickson, Jr., R. Leonard, and L. Asmussen. 1984. Riparian forest as nutrient filters in agricultural watersheds. Bioscience 34:374–377.
Nelson, W.M., A.J. Gold, and P.M. Groffman. 1995. Spatial and temporal variation in groundwater nitrate removal in a riparian forest. J. Environ. Qual. 24:691–699.
Nielsen, L.P. 1992. Denitrification in sediment determined from nitrogen isotope pairing. FEMS Microbiol. Ecol. 86:357–362.
Paludan, C., and G. Blicher-Mathiesen. 1996. Losses of inorganic carbon and nitrous oxide from a temperate freshwater wetland in relation to nitrate loading. Biogeochem. 35:305–326.
Patankar, S.V. 1980. Numerical heat transfer and fluid flow. McGraw Hill, New York.
Pavel, E.W., R.B. Reneau, Jr., D.F. Berry, E.P. Smith, and S. Mostaghimi. 1996. Denitrification potential of nontidal riparian wetland soils in the Virginia Coastal Plain. Water Res. 11:2798–2804.
Peterjohn, W.T., and D.L. Correll. 1984. Nutrient dynamics in an agricultural watershed: Observations on the role of a riparian forest. Ecology 65:1466–1475.
Pinay, G., and H. Decamps. 1988. The role of riparian woods in regulating nitrogen fluxes between the alluvial aquifer and surface water; a conceptual model. Regul. River. 2:507–516.
Pinay, G., L. Roques, and A. Fabre. 1993. Spatial and temporal patterns of denitrification in a riparian forest. J. Appl. Ecol. 30: 581–591.
Risgaard-Petersen, N., and S. Rysgaard. 1995. Nitrate reduction in sediments and waterlogged soil measured by ^{15}N techniques. p. 287–295. *In* K. Alef and P. Nannipen (ed.) Methods in applied soil microbiology and biochemistry. Academic Press, New York.
Risgaard-Petersen, N., S. Rysgaard, and N.P. Revsbech. 1993. A sensitive assay for determination of $^{14}N/^{15}N$ isotope distribution in NO_3^-. J. Microbiol. Meth. 17:155–164.
Schipper, L.A., A.B. Cooper, C.G. Harfoot, and W.J. Dyck. 1993. Regulators of denitrification in an organic riparian soil. Soil Biol. Biochem. 25:925–933.
Stepanauskas, R., E.T. Davidsson, and L. Leonardson. 1996. Nitrogen transformations in wetland soil cores measured by ^{15}N isotope pairing and dilution at four infiltration rates. Appl. Environ. Microbiol. 62:2345 2351.
Willems, H.P.L., M.D. Rotelli, D.F. Berry, E.P. Smith, R.B. Reneau, and S. Mostaghimi. 1997. Nitrate removal in riparian wetland soils: Effects of flow rate, temperature, nitrate concentration and soil depth. Water Res. 31:841–849.